MDPI

Article

Hepialiamides A–C: Aminated Fusaric Acid Derivatives and Related Metabolites with Anti-Inflammatory Activity from the Deep-Sea-Derived Fungus *Samsoniella hepiali* W7

Zheng-Biao Zou [1,2,†], Tai-Zong Wu [2,†], Long-He Yang [3], Xi-Wen He [3], Wen-Ya Liu [1], Kai Zhang [2], Chun-Lan Xie [2], Ming-Min Xie [2], Yong Zhang [2], Xian-Wen Yang [2,*] and Jun-Song Wang [1,*]

[1] Center for Molecular Metabolism, School of Environmental and Biological Engineering, Nanjing University of Science and Technology, 200 Xiaolingwei Street, Nanjing 210094, China; zhengbiaozou@njust.edu.cn (Z.-B.Z.); wenyaliu2015@163.com (W.-Y.L.)

[2] Key Laboratory of Marine Genetic Resources, Third Institute of Oceanography, Ministry of Natural Resources, 184 Daxue Road, Xiamen 361005, China; wutaizong@tio.org.cn (T.-Z.W.); z18252730063@163.com (K.Z.); xiechunlanxx@163.com (C.-L.X.); xiemingmin@tio.org.cn (M.-M.X.); zhangyong@tio.org.cn (Y.Z.)

[3] Technical Innovation Center for Utilization of Marine Biological Resources, Third Institute of Oceanography, Ministry of Natural Resources, 184 Daxue Road, Xiamen 361005, China; longheyang@tio.org.cn (L.-H.Y.); hexiwen1224@163.com (X.-W.H.)

[*] Correspondence: yangxianwen@tio.org.cn (X.-W.Y.); wang.junsong@gmail.com (J.-S.W.); Tel.: +86-592-2195319 (X.-W.Y.); +86-25-8431-5512 (J.-S.W.)

[†] These authors contributed equally to this work.

Abstract: A systematic investigation combined with a Global Natural Products Social (GNPS) molecular networking approach, was conducted on the metabolites of the deep-sea-derived fungus *Samsoniella hepiali* W7, leading to the isolation of three new fusaric acid derivatives, hepialiamides A–C (**1–3**) and one novel hybrid polyketide hepialide (**4**), together with 18 known miscellaneous compounds (**5–22**). The structures of the new compounds were elucidated through detailed spectroscopic analysis. as well as TD-DFT-based ECD calculation. All isolates were tested for anti-inflammatory activity in vitro. Under a concentration of 1 μM, compounds **8**, **11**, **13**, **21**, and **22** showed potent inhibitory activity against nitric oxide production in lipopolysaccharide (LPS)-activated BV-2 microglia cells, with inhibition rates of 34.2%, 30.7%, 32.9%, 38.6%, and 58.2%, respectively. Of particularly note is compound **22,** which exhibited the most remarkable inhibitory activity, with an IC_{50} value of 426.2 nM.

Keywords: deep-sea-derived fungus; fusaric acid derivatives; GNPS molecular networking; inflammation; nitric oxide production

1. Introduction

Secondary metabolites produced by marine-derived fungi have been proven to possess a broad spectrum of bioactivities, such as cytotoxicity, antibacterial, antioxidant, antimalarial, anti-inflammatory, and antiviral properties and have been recognized as significant chemical entities for drug discovery [1–8]. However, continuous investigations on secondary metabolites from marine-derived fungi have led to a high frequency of rediscovery of known compounds, for which, dereplication becomes critical in microbial biodiscovery. Mass spectrometry-based GNPS molecular networking (https://gnps.ucsd.edu, accessed on 1 January 2016) is a strategy that has been proven to be a powerful and promising tool for dereplication. GNPS uses an untargeted metabolomics approach that powerfully processes tandem mass spectrometry (MS/MS) fragmentation data. It is a vector-based workflow that calculates cosine scores (between 0 and 1) to determine the degree of similarity between MS^2 fragments. These fragment ions (nodes) are then organized into relational networks depending on their similarity [9–11]. GNPS has been widely used to identify

known compounds and potential new analogs, greatly speeding up the dereplication and structure-based discovery of natural products [12–14].

Fusaric acid (FA), featuring a picolinic acid core, is a well-known mycotoxin commonly found in the metabolites of numerous *Fusarium* species. The biosynthesis of FA and its related analogues has attracted attention since the last century due to the intriguing pyridine moiety, which has been proven to start from an aspartic acid precursor and malonyl-CoA [15–18]. However, naturally occurring amidated derivatives of FA have not been well-described yet in terms of their structural diversity and biological activity, with only two examples reported so far, including atransfusarin from the endophytic fungus *Alternaria atrans* MP-7 [19] and 2-(4-butylpicolinamide) acetic acid from *Fusarium fujikuroi* [20]. Atransfusarin was documented with mild anti-fungi activity while 2-(4-butylpicolinamide) acetic acid was inactive against the tested pathogens.

As part of our ongoing exploration of structurally novel and bioactive secondary metabolites from marine microbes [21–24], we performed a systematic investigation, aided by a GNPS molecular networking approach, on the crude extract of the culture of fungus *Samsoniella epialid* W7, isolated from the sulfide at a depth of 3073 m in the South Atlantic. Prior to isolation, the GNPS network of the extract revealed a big molecular cluster within which none of the nodes were identified by the internal compound library (Figure 1), indicating a certain possibility of new compounds to be found among these metabolites. A further scrutiny of their MS/MS fragmentation pattern (Figure S29), followed by HRMS-based molecular formula analysis, strongly suggested that they were new analogues of fusaric amides [20]. The systematic isolation, along with targeted purification, finally yielded three new fusaric acids, hepialiamides A–C (**1**–**3**), and one novel hybrid polyketide, hepialide (**4**), together with 18 known compounds (**5**–**22**) (Figure 2). The known compounds **8**, **11**, **13**, **21**, and **22** exhibited inhibitory activity against LPS-induced NO production. Herein, we report the fermentation, isolation, structure characterization and bioactivity of these isolates.
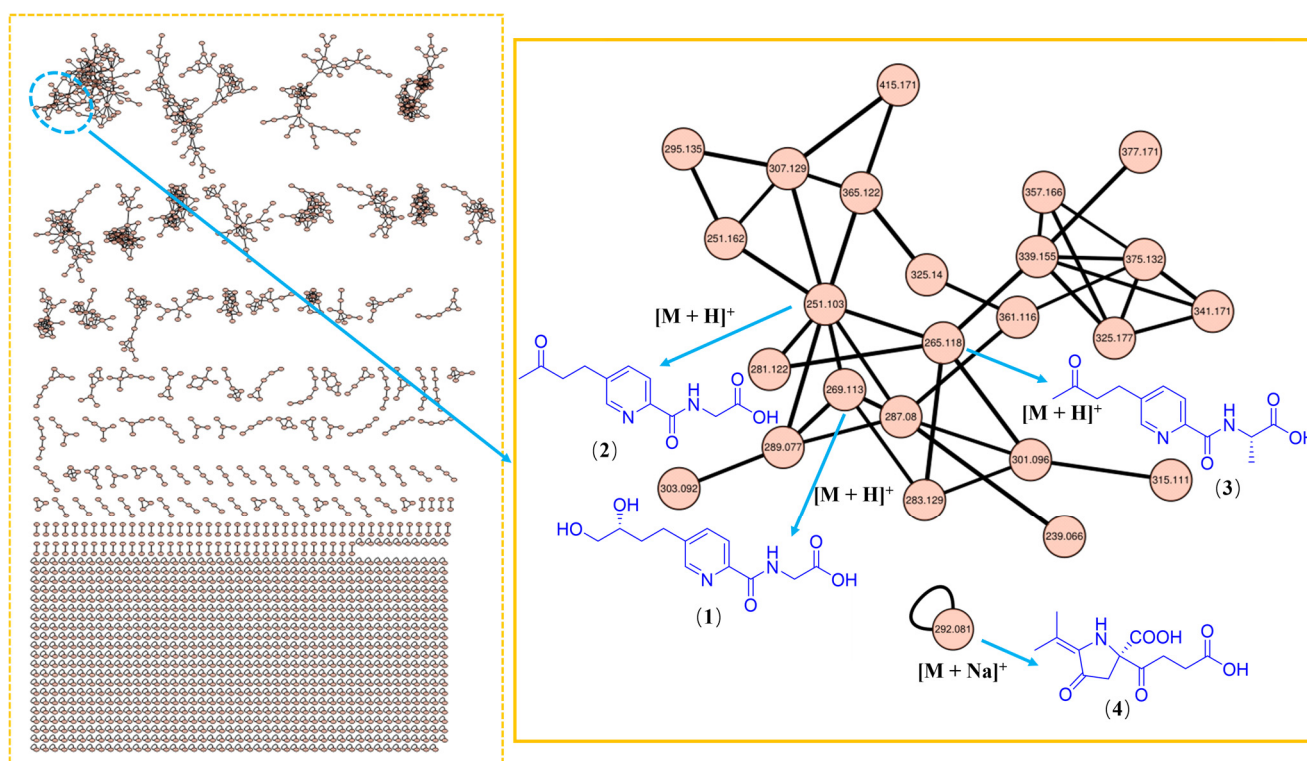

Figure 1. Molecular network of extract of the fungus *Samsoniella hepiali* W7. The cluster of new compounds (**1**–**4**) is expanded, and the nodes are marked with the *m/z* value of the parent ion.
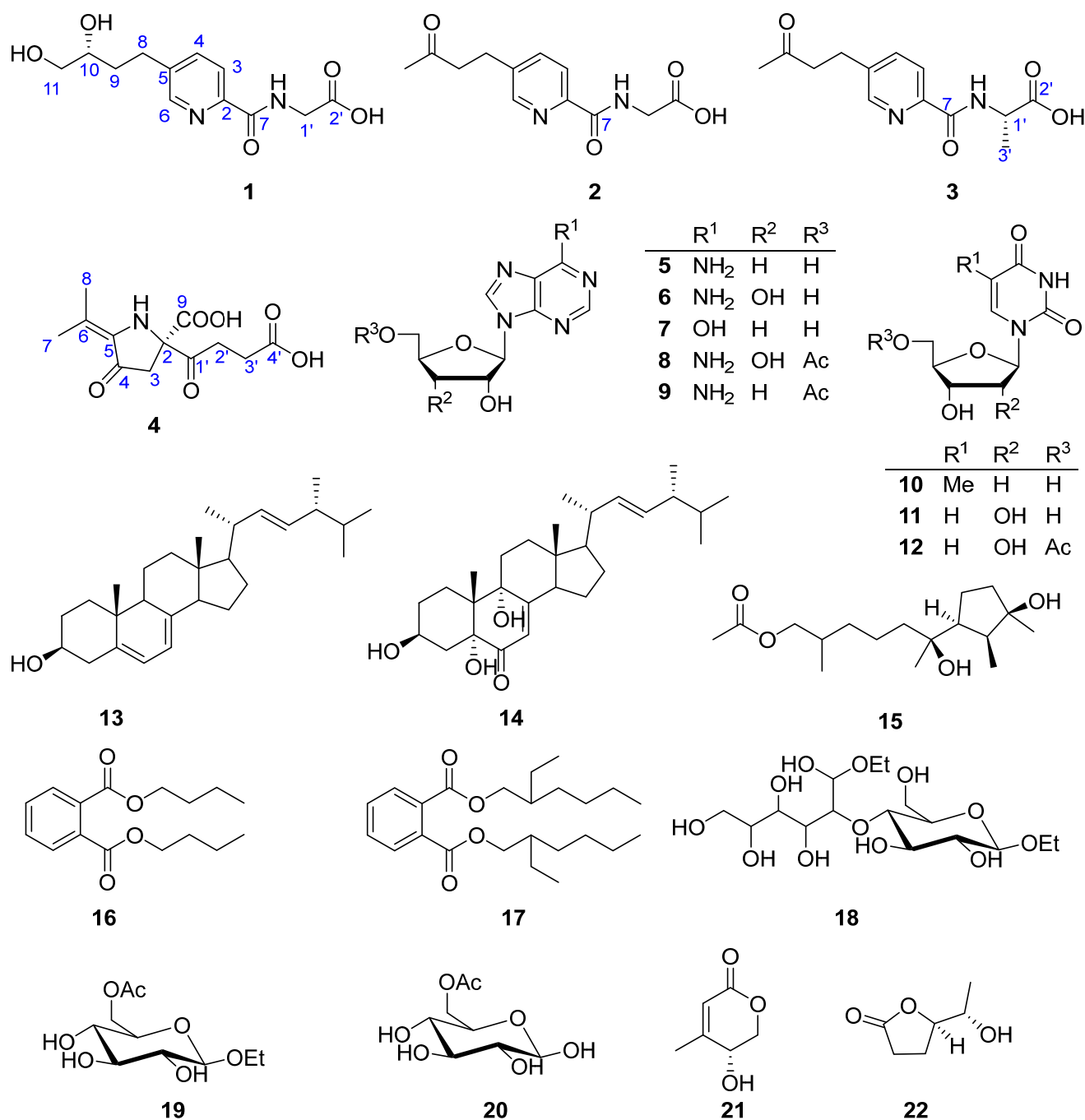
Figure 2. Compounds **1**–**22** from *Samsoniella hepiali* W7.

2. Results and Discussion

Compound **1** was isolated as a yellow oil. The HRESI(+)MS of **1** exhibited a protonated molecular ion [M + H]$^+$ at *m/z* 269.1142, indicating a molecular formula of $C_{12}H_{17}N_2O_5$, accounting for seven degrees of unsaturation (DoU). The ^{1}H NMR (Table 1) data of **1** presented the diagnostic signals of three aromatic protons, typically an ABX coupling system at δ_H 8.51 (1H, d, *J* = 1.5 Hz, H-6), 7.96 (1H, d, *J* = 8.0 Hz, H-3), and 7.83 (1H, dd, *J* = 8.0, 2.0 Hz, H-4), indicating the presence of a 2,5-disubstituted pyridine ring in **1**. This was confirmed by the key heteronuclear multiple bond correlation (HMBC) cross-peaks from H-3 to C-5 (δ_C 141.4), from H-4 to C-2 (δ_C 147.3) and C-6 (δ_C 148.5), and from H-6 to C-2 and C-4 (δ_C 137.4), as well as by the correlation spectroscopy (COSY) correlations of H-3/H-4.

Table 1. ^{1}H (400 Hz) and ^{13}C NMR (100 Hz) spectroscopic data of compounds **1–3**.

No.	1 [a] (δ_C, Type)	1 [a] (δ_H, Mult J in Hz)	2 [b] (δ_C, Type)	2 [b] (δ_H, Mult J in Hz)	3 [a] (δ_C, Type)	3 [a] (δ_H, Mult J in Hz)
2	147.3, C		148.4, C		147.4, C	
3	121.7, CH	7.96, d (8.0)	122.8, CH	7.96, d (8.0)	121.6, CH	7.93, d (7.6)
4	137.4, CH	7.83, dd (2.0, 8.0)	138.3, CH	7.77, dd (2.0, 8.0)	137.4, CH	7.82, d (8.0)
5	141.4, C		141.9, C		141.3, C	
6	148.5, CH	8.51, d (1.5)	150.1, CH	8.47, d (1.6)	148.7, CH	8.51, s
7	164.2, C		167.0, C		163.5, C	
8	28.3, CH$_2$	2.71, m; 2.82, m	27.5, CH$_2$	2.90, d (5.2)	26.1, CH$_2$	2.85, m
9	34.7, CH$_2$	1.56, m; 1.77, m	44.6, CH$_2$	2.88, d (5.2)	43.3, CH$_2$	2.84, m
10	70.2, CH	3.39, m	209.8, C		207.3, C	
11	65.8, CH$_2$	3.25, dd (5.7, 10.7) 3.32, dd (5.6, 10.7)	29.9, CH$_3$	2.13, s	29.7, CH$_3$	2.09, s
1'	41.0, CH$_2$	3.97, s	41.9, CH$_2$	4.15, s	47.6, CH	4.46, d (7.1)
2'	171.1, C		172.8, C		173.8, C	
3'					17.5, CH$_3$	1.42, d (7.1)
NH		8.92, t (6.0)		9.04, t (5.4)		8.74, d (7.3)

[a] Measured in DMSO-d_6. [b] Measured in methanol-d_4.

Furthermore, four methylene groups at δ_H 3.97 (2H, s, H-1'), [2.71 (1H, m, H-8), 2.82 (1H, m, H-8)] and [1.56 (1H, m, H-9), 1.77 (1H, m, H-9)], [3.25 (1H, dd, J = 10.7, 5.7 Hz, H-11), 3.32 (1H, dd, J = 10.7, 5.6 Hz, H-11)] and one oxymethine at δ_H 3.39 (1H, m, H-10), were observed (Table 1). The ^{1}H-^{1}H COSY correlations of H-8/H-9/H-10/H-11, together with the HMBC correlations from H-11 to C-10 (δ_C 70.2) and C-9 (δ_C 34.7), from H-10 to C-9 and C-8 (δ_C 28.3), from H-9 to C-8 and C-5, and from H-8 to C-4, C-5, and C-6 indicated a 1,2-butanediol moiety at C-5. Further HMBC correlations of H-1' to C-7 (δ_C 164.2) and C-2' (δ_C 171.1) suggested the presence of a glycine moiety (Figure 3). An amido bond between C-2 of the pyridine ring and C-1' of the glycine unit was confirmed by key HMBC correlations from H-3 and H-1' to C-7. Thus, compound **1** was identified as a new fusaric acid derivative and given the trivial name hepialiamide A. The comparison of its optical rotation value ($[\alpha]_D^{25}$ + 13) with those of similar known compounds, such as (*R*)-4-phenyl-1,2-butanediol ($[\alpha]_D^{20}$ + 33) and (*S*)-4-phenyl-1,2-butanediol ($[\alpha]_D^{20}$ − 34) [25], and comparative analysis of the experimental and theoretically calculated ECD curves established the absolute configuration of hepialiamide A to be 10*R* (Figure 4).
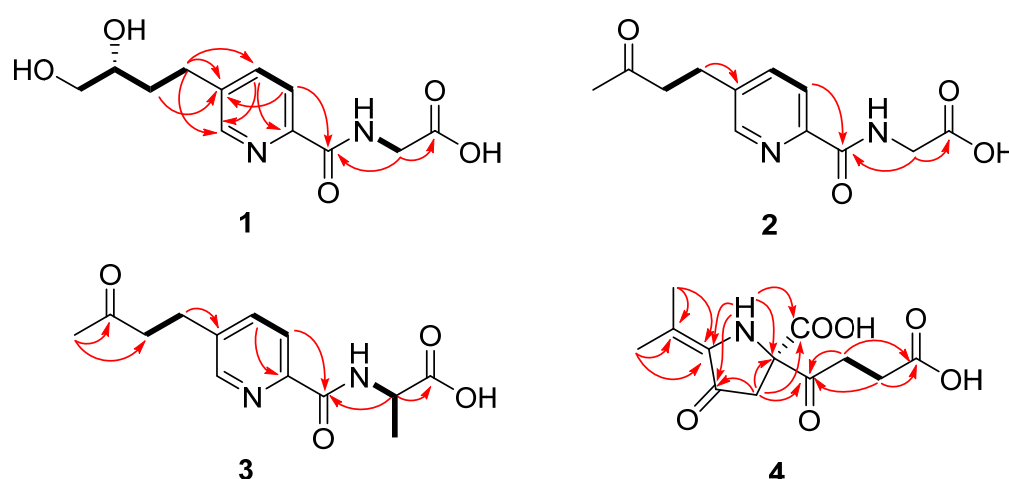
Figure 3. Key HMBC (arrows) and ^{1}H–^{1}H COSY (bold) correlations of compounds **1–4**.

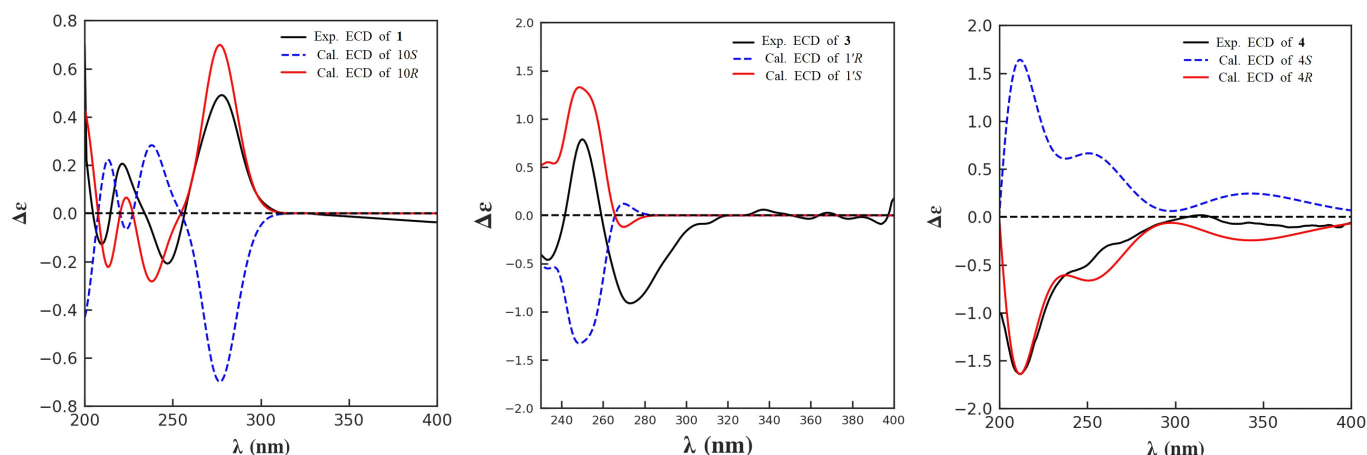**Figure 4.** Experimental and calculated ECD spectra of **1**, **3**, and **4**.

Compound **2** was isolated as a yellow oil. The HRESI(+)MS of **2** exhibited a protonated molecular ion $[M + H]^+$ at m/z 251.0950. Analysis of the HRESI(+)MS and ^{13}C NMR data revealed the molecular formula $C_{12}H_{14}N_2O_4$ of **2** indicating seven DoUs. The NMR data (Table 1) of **2** were closely related to those of **1**, except for the presence of a methyl ketone group at (δ_C 209.8, C-10) and (δ_C 29.9, δ_H 2.13, CH$_3$-11) in **2**, which was supported by the HMBC correlations of H$_3$-11 to C-10 and C-9 (δ_C 44.6). The left of the structure was confirmed by 2D NMR correlations, as shown (Figure 3). Therefore, **2** was identified as a new analogue of **1** and named hepialiamide B.

Compound **3** was obtained as a yellow oil with the molecular formula of $C_{13}H_{16}N_2O_4$ implied by its HRESI(+)MS spectrum. The 1D NMR data (Table 1) of **3** were similar to those of **2** except that **3** had an extra methyl group [δ_C 18.2 (C-4′)] at C-2′, which was confirmed by the COSY correlations of NH (δ_H 8.74, d)/H-1′ (δ_H 4.46, d)/H-3′ (δ_H 1.42, d) and the HMBC correlations from H-1′ to C-2′ (δ_C 173.8), C-3′ (δ_C 17.5), and C-7 (δ_C 163.5). The absolute configuration of the chiral center C-1′ in **3** was established to be *S*, as indicated by the agreement between the calculated ECD spectrum of **3** and the experimental data (Figure 4). Hence, compound **3** was identified as another new fusaric acid derivative, and named hepialiamide C.

Compound **4** was obtained as a yellow oil. The HRESI(+)MS of **4** exhibited a sodiated molecular ion $[M + Na]^+$ at m/z 292.0800, suggesting a molecular formula (calculated for $C_{12}H_{15}NO_6Na$, 292.0797) that requires six DoUs. The ^1H NMR (Table 2) data of **4** presented the diagnostic signals of three methylene groups at δ_H 2.28 (2H, t, *J* = 6.3 Hz, H-2′), 2.64 (2H, q, *J* = 6.9 Hz, H-3′), and 3.10 (2H, q, *J* = 15.0 Hz, H-3), and two methyl groups at 2.08 (3H, s, H-8) and 1.81 (3H, s, H-9). In the ^{13}C NMR spectrum, 12 carbon signals were observed and classified as two methyl (δ_C 20.8, 18.5), three methylene (δ_C 47.4, 36.3, 27.4), and seven non-protonated carbons (δ_C 207.2, 197.0, 173.5, 171.4, 1129.1, 122.3, 70.3), with the aid of HSQC data. In the ^1H-^1H COSY spectrum of **4**, homonuclear vicinal coupling correlation (Figure 3) between H-7 and H-8, along with the HMBC correlations from H-7 to C-5/6, from H-8 to C-5/6, indicated an isopropenyl group. The HMBC cross-peaks observed from H-3 to C-2/4/9, H-7/8 to C-4, and the diagnostic signals from an exchangeable proton to C-2/4/5/9 permitted the construction of a five-member ring. Finally, based on the rest of the HMBC correlations from H-3 to C-1′, H-2′ to C-1′/3′/4′, from H-3′ to C-1′/4′, and the COSY signals between H-2′ to H-3′, together with a comparable analysis of the chemical shifts of C-2/5 in **4** and those in literature [26,27], the planar structure o f **4** was assigned as shown.

Table 2. ^{1}H (400 Hz) and ^{13}C (100 Hz) NMR spectroscopic data of compound **4** in DMSO-d_6.

No.	δ_C, Type	δ_H, Mult (*J* in Hz)
2	70.3, C	
3	47.4, CH$_2$	3.15, d (18.0); 3.06, d (18.0)
4	197.0, C	
5	122.3, C	
6	129.1, C	
7	18.5, CH$_3$	2.08, s
8	20.8, CH$_3$	1.81, s
9	171.4, C	
1′	207.2, C	
2′	27.4, CH$_2$	2.28, t (6.3)
3′	36.3, CH$_2$	2.68, m; 2.60, m
4′	173.5, C	
NH		10.27, s

To further assign the absolute configuration of C-2, a theoretical calculation of the ECD spectra of the 4*R*- and 4*S*-isomers was conducted. The experimental ECD spectrum of **4** was in good accordance with the calculated result for the 4*R*-configured **4** (Figure 4). The structure of compound **4** was thus determined and named hepialide.

By comparing the NMR, MS, ECD, and OR data with those reported in the references, 18 previously described components were identified as cordycepin (**5**) [28], adenosine (**6**) [29], 3′-deoxyinosine (**7**) [30], 5′-*O*-acetyladenosine (**8**) [31], 5′-acetyl-3′-deoxyadenosine (**9**) [32], thymidine (**10**) [33], uridine (**11**) [34], 5′-*O*-acetyluridine (**12**) [35], ergosterol (**13**) [36], 3*β*,5*α*,9*α*-trihydroxyergosta-7,22-diene-6-one (**14**) [37], 12-acetoxycycloneran-3,7-diol (**15**) [38], dibutyl phthalate (**16**) [39], di-(2-ethylhexyl)phthalate (**17**) [40], oryzasaccharide A (**18**) [41], D-glucopyranoside, ethyl, 6-acetate (**19**) [42], 6-O-acetyl-D-glucose (**20**) [43], walterolactone A (**21**) [44], and (4*R*,5*S*)-5-hydroxyhexan-4-olide (**22**) [45]. Among them, **16** and **17** were previously described as plasticizers and common contaminants in natural products [46].

Naturally occurring aminated fusaric acid derivatives are uncommon in fungal metabolites, as mentioned above. Hepialiamides A–C (**1**–**3**) feature an oxidized fusaric acid core structure with a glycine or alanine coupled through an amide bond, representing the third examples of fusaric amides of fungal origin. Hepialide is a novel PKS-NRPS hybrid polyketide with an unusual isopropenylated pyrrolidone moiety that resembles the tetramic acid.

Neuroinflammation, characterized by the activation of microglia cells, is a common denominator in diverse neurological conditions, including neurodegenerative diseases, traumatic brain injury, and neuroinfectious disorders. Microglia cell activation contributes significantly to the progression of these diseases by releasing pro-inflammatory mediators, exacerbating neuronal damage and impairing synaptic plasticity [47]. Hence, inhibiting glial cell activation emerges as a promising therapeutic strategy. The rich diversity and unique chemical structures of marine compounds provide a vast pool of potential drugs. Inflammatory tests were conducted on BV-2 microglia cells. Stimulation of the cells with bacterial products like lipopolysaccharide (LPS) triggers the production of NO and pro-inflammatory cytokines, key mediators in inflammation [48]. Given the significance of high NO levels in inflammation, targeting inducible nitric oxide synthase (iNOS), the enzyme responsible for NO synthesis, has been suggested as an anti-inflammatory therapeutic approach.

In this LPS-induced BV-2 microglia cell model, we evaluated the inhibitory activity of these compounds on NO production at a low concentration (1 μM). The cells were pre-exposed to the compounds for 1 h, followed by LPS stimulation for 24 h, and subsequently, the concentration of nitrite, the primary metabolite derived from NO, was quantified. The results indicated that compounds **8**, **11**, **13**, **21**, and **22** reduced NO production by 34.2 ± 1.6%, 30.7 ± 4.8%, 32.9 ± 1.6%, 38.6 ± 2.1%, and 58.2 ± 2.6%, respectively, with

respect to vehicle-treated stimulated cells (Figure 5A). Particularly noteworthy, further analysis revealed that compound **22** exhibited a remarkable dose-dependent inhibitory effect, with an IC_{50} value of 426.2 nM (Figure 5B).
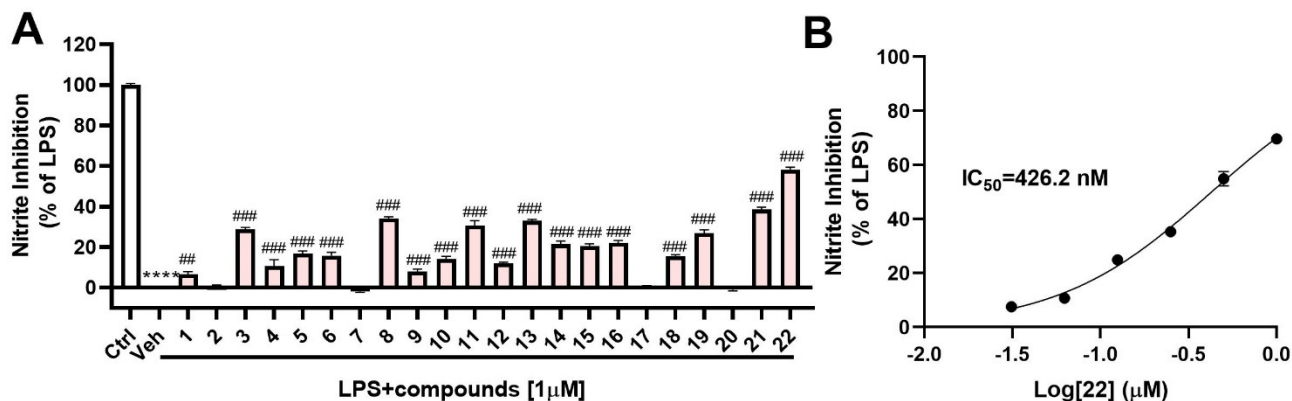

Figure 5. The impact of compounds on NO release in LPS-induced microglia cells: (**A**) Nitrite accumulation in the culture media was quantified using the Griess method, and nitrite production inhibition was calculated compared to the only LPS treated group. Results were normalized to the LPS condition and presented as mean $\pm$ SEM (n = 4); **** $p < 0.0001$ vs. Ctrl; ### $p < 0.0001$, ## $p < 0.01$ vs. Veh; (**B**) Inhibitory curve of compound **22** against nitrite production.

These compounds, especially compound **22**, frequently demonstrate anti-inflammatory and immunomodulatory properties, rendering them promising candidates for the development of specific and potent inhibitors that target microglia cell activation pathways. Further research is needed for in-depth evaluation.

3. Materials and Methods

3.1. General Experimental Procedures

Optical rotations were recorded on a Rudolph IV Autopol automatic polarimeter at 25 °C. NMR spectra, including ^{1}H, ^{13}C, DEPT, HSQC, COSY, HMBC, and NOESY were measured on a Bruker Avance 400 MHz spectrometer. Chemical shifts were recorded in δ values using solvent signals (DMSO-d_6: δ_H 2.50/δ_C 39.5; methanol-d_4: δ_H 3.31/δ_C 49.0; CDCl$_3$: δ_H 7.27/δ_C 77.0) as references. HRESIMS data were measured on a Xevo G2 Q-TOF mass spectrometer (Waters Corporation, Milford, MA, USA). Preparative and semipreparative HPLC were performed on an Agilent Technologies 1260 infinity instrument equipped with the DAD detector. UV spectra were recorded on a UV-8000 UV/Vis spectrometer (Shanghai Yuanxi Instrument Co., Ltd., Shanghai, China). Column chromatography (CC) was performed on ODS (50 μm, Daiso, Hiroshima, Japan), silica gel (Qingdao Marine Chemistry Co., Ltd., Qingdao, China), and Sephadex LH-20 (Amersham Pharmacia Biotech AB, Uppsala, Sweden). The TLC plates were visualized under UV light or by spraying with 10% H$_2$SO$_4$. Solvents for isolation were analytical grade. HRMS and MS/MS data were acquired with ultra-high performance liquid chromatography–quadrupole time-of-flight mass spectrometry (UHPLC-Q-TOF MS, AB SCIEX Triple TOF 5600$^+$, Waters Corporation, Milford, MA, USA), with a Phenomenex Kinetex® C18 (100 × 2.1 mm, 2.6 μm).

3.2. Fungal Identification, Fermentation, and Extract

The strain W7 was isolated from a sulfide sample (W 14.52°, S 13.59°) at a depth of 3073 m from the South Atlantic. It was identified as *Samsoniella hepiali* (GenBank accession number OR398925), as the ITS DNA gene sequence alignment demonstrated its similarity to *Samsoniella hepiali* CGMCC 3.17103 (GenBank accession number NR_160318.1). The strain is preserved at the Key Laboratory of Marine Biogenetic Resources, Third Institute of Oceanography, Ministry of Natural Resources (Xiamen, China). The strain *Samsoniella hepiali* was cultured on a PDA plate at 25 °C for 3 days. Fresh mycelia and spores were inoculated

into 250 mL Erlenmeyer flasks ($\times$10) containing 30 mL PDB medium and incubated in a 180 rpm rotary shaker at 28 °C for 5 days. Then, the spore cultures were used to inoculate 25 $\times$ 1 L Erlenmeyer flasks containing rice medium (80 g rice and 120 mL distilled H_2O for each flask) to perform large-scale fermentation. After 25 days, the fermented culture was extracted with EtOAc three times to provide a crude extract. The extract was redissolved in MeOH and extracted with petroleum ether (PE) three times. The MeOH solution was evaporated under reduced pressure to obtain a defatted extract (25 g).

3.3. UHPLC-Q-TOF and Molecular Networking Analysis

The crude extract was analyzed by LC-MS/MS, equipped with an Atlantis$^{\text{TM}}$ Premier BEH C$_{18}$ AX (2.1 $\times$ 100 mm, 1.7 μm) column. Samples were dissolved in MeOH with 1 mg/mL. A 10 μL aliquot of each sample was injected and eluted, using a gradient program with water + 0.1% formic acid (A) and CH_3CN + 0.1% formic acid (B). The elution started with a 1% B isocratic phase for 1 min, followed by a gradient from 1% to 99% B in 10 min, maintaining 99% B for 3 min. Then, a gradient from 99% to 1% B in 1 min was applied, and 1% B was maintained for 3 min at a flow rate of 0.4 mL/min, with the temperature maintained at 40 °C. The full mass spectrometry (MS) survey scan was performed in positive electrospray ionization (ESI) mode within the range of 50 to 1000 Da. The MS/MS data were converted to mzXML files using MSConvert software (version 3.01). The converted MS/MS file was submitted to the GNPS platform for molecular networking for dereplication (https://gnps.ucsd.edu, accessed on 1 January 2016). Parameters for molecular network generation were set as follows: both precursor mass and MS/MS fragment ion tolerance were set at 0.02 Da, minimum pairs cosine score 0.6, minimum matched fragment ions 6, minimum cluster size 2, network TopK 10. The spectral networks were imported into Cytoscape 3.9.1 and visualized using the force-directed layout.

3.4. Isolation and Purification

The MeOH extract (25 g) was subjected to CC over silica gel using sequential gradient elution with CH_2Cl_2-MeOH (100:1, 50:1, 30:1, 20:1, 10:1, 5:1, 2:1, and 0:1) to obtain five fractions (Fr.1–Fr.5), based on TLC properties. Fraction Fr.1 (5 g) was chromatographed over ODS using gradient elution of MeOH-H_2O (30 → 80%) to get five subfractions (Fr.1-1–Fr.1-5). Fr.1-1 (625 mg) was subjected to CC on Sephadex LH-20 (MeOH), followed by repeated CC over silica gel, using gradient PE-EtOAc (3:1 → 1:1) to yield **17** (125 mg) and **2** (62 mg). Fr.1-2 (34 mg) was directly separated by Sephadex LH-20 (MeOH) to yield **15** (2 mg). Fr.1-3 (215 mg) was subsequently separated by CC over Sephadex LH-20 (MeOH), silica gel (CH_2Cl_2-MeOH, 100:1 → 50:1), and preparative TLC (PTLC) (CH_2Cl_2-MeOH, 20:1) to obtain **22** (14 mg) and **21** (2 mg). Fr.1-4 (137 mg) was subjected to CC over Sephadex LH-20 (MeOH) and silica gel (CH_2Cl_2-MeOH, 75:1) to yield **3** (40 mg). Fr.1-5 (226 mg) was purified by CC over Sephadex LH-20 (MeOH), silica gel (CH_2Cl_2-MeOH, 100:1), and preparative TLC (PTLC) (CH_2Cl_2-MeOH, 100:1) to afford compound **14** (7 mg).

Fraction Fr.2 (1.3 g) was subjected to CC over ODS with MeOH-H_2O (2% → 30%), followed by purification using CC on Sephadex LH-20 (MeOH), crystallization (MeOH), and silica gel (EtOAc-MeOH, 20:1 → 5:1) to yield **20** (84 mg), **18** (29 mg), 5 (46 mg), **6** (5 mg), **10** (11 mg), **7** (7 mg), **1** (15 mg), and **11** (26 mg).

Fraction Fr.3 (1.5 g) was subjected to CC over ODS with MeOH-H_2O (2% → 50%) and CC on Sephadex LH-20 (MeOH) to yield **19** (4 mg), **4** (11 mg), **12** (11 mg), and **8** (4 mg).

Fraction Fr.4 (9.8 g) was separated by CC over silica gel using sequential gradient elution with PE-EtOAc (100:1, 50:1, 30:1, 20:1, 10:1) and Sephadex LH-20 (CH_2Cl_2-MeOH, 1:1) to yield **13** (320 mg).

Fraction Fr.5 (5.3 g) was subjected to CC over ODS with MeOH-H_2O (10% → 50%), followed by purification using CC on Sephadex LH-20 (MeOH), HPLC (20% → 48%, MeOH-H_2O), crystallization (MeOH), and silica gel (EtOAc-MeOH, 20:1) to yield **9** (2 mg) and **16** (4 mg).

Hepialiamide A (**1**): Yellow oil; $[\alpha]_D^{25}$ + 13 (c 0.10, MeOH), ECD (MeOH) λmax (Δε) 278 (0.07), 245 (−0.09), 217 (0.07); UV (MeOH) λmax (log ε) 229 (2.72), 269 (2.31) nm; HRESIMS m/z 269.1142 [M + H]$^+$ (calcd for $C_{12}H_{17}N_2O_5$, 269.1137).

Hepialiamide B (**2**): Yellow oil; UV (MeOH) λmax (log ε) 230 (2.76), 269 (2.38) nm; ^{1}H and ^{13}C NMR data, Table 1; HRESIMS m/z 251.0950 [M + H]$^+$ (calcd for $C_{12}H_{15}N_2O_4$, 251.1032).

Hepialiamide C (**3**): Yellow oil; $[\alpha]_D^{25}$ + 3 (c 0.10, MeOH); ECD (MeOH) λmax (Δε) 275 (−0.15), 250 (0.13), 213 (−0.17); UV (MeOH) λmax (log ε) 200 (3.06), 269 (2.23) nm; HRESIMS m/z 265.111 [M + H]$^+$ (calcd for $C_{13}H_{17}N_2O_4$, 265.1188).

Hepialide (**4**): Yellow oil; $[\alpha]_D^{25}$ + 5 (c 0.10, MeOH); ECD (MeOH) λmax (Δε) 211 (−0.28); UV (MeOH) λmax (log ε) 228 (2.53), 291 (1.91) nm; HRESIMS m/z 292.0800 [M + Na]$^+$ (calcd for $C_{12}H_{15}NO_6Na$, 292.0797).

3.5. Theoretical ECD Calculation

As reported previously, conformational analysis was first performed via random searching in Sybyl-X 2.0 using the MMFF94S force field with an energy cutoff of 7.0 kcal/mol and an RMSD threshold of 0.2 Å. All conformers were consecutively optimized at PM6 and HF/6-31G(d) levels. Dominant conformers were re-optimized at the B3LYP/6-31G(d) level in the gas phase. The theoretical ECD spectra were calculated using the GIAO method at the MPW1PW91/6-31G (d, p) level in MeOH using Gaussian 09. The ECD spectrum was simulated in SpecDis (version 1.71) by overlapping Gaussian functions for each transition.

3.6. BV-2 Cell Culture and Treatment

BV-2 microglia cells were cultured in DMEM medium containing 10% fetal bovine serum and antibiotics (100 units/mL of penicillin and 100 g/mL of streptomycin) and maintained in a humidified 5% CO_2 incubator at 37 °C. For the experiment, cells were seeded overnight into 24-wells with 2×10^4 cells per well. The next day, cells were incubated with fresh culture medium containing the indicated concentration of compounds for an hour, followed by lipopolysaccharides (LPS) treatment (1 μg/mL). Cells treated with the vehicle (DMSO, 0.1%) served as the control.

3.7. Nitrite Quantification

The concentration of nitrite in the culture medium was determined using the Griess Reagent Kit (Therofisher, Shanghai, China). Briefly, 75 μL of cell culture supernatants was reacted with an equal volume of the Griess Reagent Kit for 30 min at room temperature, and the absorbance of the diazonium compound was obtained at a wavelength of 560 nm. Nitrite production by vehicle stimulation was designated as 100% inhibition (Ctrl) compared to LPS stimulation (Veh) for the experiment.

4. Conclusions

In summary, three new aminated fusaric acid derivatives, hepialiamides A–C (**1–3**), and one novel hybrid polyketide, hepialide (**4**), together with 18 known miscellaneous compounds (**5–22**), were isolated from the cultures of the deep-sea-derived fungus *Samsoniella hepiali* W7 with the aid of GNPS molecular networking. Hepialiamides A–C feature a glycine/alanine unit embedded in the fusaric acid backbone, representing the third examples of naturally occurring fusaric amides, while hepialide features an uncommon isopropenylated pyrrolidone moiety. Biologically, compound **8**, **11**, **13**, **21,** and **22** showed more than 30% inhibition against NO production induced by LPS at 1 μM, with **22** exhibiting a particularly low nanomole IC$_{50}$, suggesting potential for developing potent anti-inflammatory drugs.

Supplementary Materials: The following are available online at https://www.mdpi.com/article/10.3390/md21110596/s1. Figures S1–S52: One-dimensional and two-dimensional NMR, UV spectra, ECD calculation details of compounds **1–4**, proton NMR spectra of **5–22**.

References

1. Newman, D.J.; Cragg, G.M. Natural products as sources of new drugs over the nearly four decades from 01/1981 to 09/2019. *J. Nat. Prod.* **2020**, *83*, 770–803. [CrossRef] [PubMed]
2. Haque, N.; Parveen, S.; Tang, T.; Wei, J.; Huang, Z. Marine natural products in clinical use. *Mar. Drugs* **2022**, *20*, 528. [CrossRef] [PubMed]
3. Teng, Y.F.; Xu, L.; Wei, M.Y.; Wang, C.Y.; Gu, Y.C.; Shao, C.L. Recent progresses in marine microbial-derived antiviral natural products. *Arch. Pharm. Res.* **2020**, *43*, 1215–1229. [CrossRef] [PubMed]
4. Carroll, A.R.; Copp, B.R.; Davis, R.A.; Keyzers, R.A.; Prinsep, M.R. Marine natural products. *Nat. Prod. Rep.* **2021**, *38*, 362–413. [CrossRef]
5. Hai, Y.; Cai, Z.M.; Li, P.J.; Wei, M.Y.; Wang, C.Y.; Gu, Y.C.; Shao, C.L. Trends of antimalarial marine natural products: Progresses, challenges and opportunities. *Nat. Prod. Rep.* **2022**, *39*, 969–990. [CrossRef]
6. Hafez Ghoran, S.; Taktaz, F.; Ayatollahi, S.A.; Kijjoa, A. Anthraquinones and their analogues from marine-derived fungi: Chemistry and biological activities. *Mar. Drugs* **2022**, *20*, 474. [CrossRef] [PubMed]
7. Carroll, A.R.; Copp, B.R.; Davis, R.A.; Keyzers, R.A.; Prinsep, M.R. Marine natural products. *Nat. Prod. Rep.* **2022**, *39*, 1122–1171. [CrossRef]
8. Carroll, A.R.; Copp, B.R.; Davis, R.A.; Keyzers, R.A.; Prinsep, M.R. Marine natural products. *Nat. Prod. Rep.* **2023**, *40*, 275–325. [CrossRef]
9. Yang, J.Y.; Sanchez, L.M.; Rath, C.M.; Liu, X.; Boudreau, P.D.; Bruns, N.; Glukhov, E.; Wodtke, A.; de Felicio, R.; Fenner, A.; et al. Molecular networking as a dereplication strategy. *J. Nat. Prod.* **2013**, *76*, 1686–1699. [CrossRef] [PubMed]
10. Nothias, L.F.; Petras, D.; Schmid, R.; Duhrkop, K.; Rainer, J.; Sarvepalli, A.; Protsyuk, I.; Ernst, M.; Tsugawa, H.; Fleischauer, M.; et al. Feature-based molecular networking in the GNPS analysis environment. *Nat. Methods* **2020**, *17*, 905–908. [CrossRef] [PubMed]
11. Aron, A.T.; Gentry, E.C.; McPhail, K.L.; Nothias, L.F.; Nothias-Esposito, M.; Bouslimani, A.; Petras, D.; Gauglitz, J.M.; Sikora, N.; Vargas, F.; et al. Reproducible molecular networking of untargeted mass spectrometry data using GNPS. *Nat. Protoc.* **2020**, *15*, 1954–1991. [CrossRef]
12. Wei, X.; Su, J.C.; Hu, J.S.; He, X.X.; Lin, S.J.; Zhang, D.M.; Ye, W.C.; Chen, M.F.; Lin, H.W.; Zhang, C.X. Probing indole diketopiperazine-based hybrids as environmental-induced products from *Aspergillus* sp. EGF 15-0-3. *Org. Lett.* **2022**, *24*, 158–163. [CrossRef] [PubMed]
13. Ding, W.J.; Tian, D.M.; Chen, M.; Xia, Z.X.; Tang, X.Y.; Zhang, S.H.; Wei, J.H.; Li, X.N.; Yao, X.S.; Wu, B.; et al. Molecular networking-guided isolation of cyclopentapeptides from the hydrothermal vent sediment derived fungus *Aspergillus pseudoviridinutans* TW58-5 and their anti-inflammatory effects. *J. Nat. Prod.* **2023**, *86*, 1919–1930. [CrossRef] [PubMed]
14. Wang, Y.; Yang, J.; Hu, L.; Bai, R.; Wang, T.; Xing, X.; Chen, L.; Ding, G. LC-MS/MS-guided molecular networking for targeted discovery of undescribed and bioactive ophiobolins from *Bipolaris eleusines*. *J. Agric. Food Chem.* **2023**, *71*, 11982–11992. [CrossRef] [PubMed]
15. Dobson, T.A.; Desaty, D.; Brewer, D.; Vining, L.C. Biosynthesis of fusaric acid in cultures of *Fusarium oxysporum Schlecht*. *Can. J. Biochem.* **1967**, *45*, 809–823. [CrossRef]
16. Stipanovic, R.D.; Wheeler, M.H.; Puckhaber, L.S.; Liu, J.; Bell, A.A.; Williams, H.J. Nuclear magnetic resonance (NMR) studies on the biosynthesis of fusaric acid from *Fusarium oxysporum* f. sp. *vasinfectum*. *J. Agric. Food Chem.* **2011**, *59*, 5351–5356. [CrossRef] [PubMed]
17. Studt, L.; Janevska, S.; Niehaus, E.M.; Burkhardt, I.; Arndt, B.; Sieber, C.M.; Humpf, H.U.; Dickschat, J.S.; Tudzynski, B. Two separate key enzymes and two pathway-specific transcription factors are involved in fusaric acid biosynthesis in *Fusarium fujikuroi*. *Environ. Microbiol.* **2016**, *18*, 936–956. [CrossRef] [PubMed]

18. Hai, Y.; Chen, M.; Huang, A.; Tang, Y. Biosynthesis of mycotoxin fusaric acid and application of a PLP-dependent enzyme for chemoenzymatic synthesis of substituted l-pipecolic acids. *J. Am. Chem. Soc.* **2020**, *142*, 19668–19677. [CrossRef] [PubMed]

19. Yang, Z.; Dan, W.J.; Li, Y.X.; Peng, G.R.; Zhang, A.L.; Gao, J.M. Antifungal metabolites from *Alternaria atrans*: An endophytic fungus in *Psidium guajava*. *Nat. Prod. Commun.* **2019**, *14*, 1934578X19844116. [CrossRef]

20. Hilário, F.; Chapla, V.M.; Araujo, A.R.; Sano, P.T.; Bauab, T.M.; dos Santos, L.C. Antimicrobial screening of endophytic fungi isolated from the aerial parts of *Paepalanthus chiquitensis* (Eriocaulaceae) led to the isolation of secondary metabolites produced by *Fusarium fujikuroi*. *J. Braz. Chem. Soc.* **2016**, *28*, 1389–1395. [CrossRef]

21. Zou, Z.B.; Chen, L.H.; Hu, M.Y.; Xu, L.; Hao, Y.J.; Yan, Q.X.; Wang, C.F.; Xie, C.L.; Yang, X.W. Cladosporioles A and B, two new indole derivatives from the deep-sea-derived fungus *Cladosporium cladosporioides* 170056. *Chem. Biodivers.* **2022**, *19*, e202200538. [CrossRef]

22. Zou, Z.B.; Zhang, G.; Zhou, Y.Q.; Xie, C.L.; Xie, M.M.; Xu, L.; Hao, Y.J.; Luo, L.Z.; Zhang, X.K.; Yang, X.W.; et al. Chemical constituents of the deep-sea-derived *Penicillium citreonigrum* MCCC 3A00169 and their antiproliferative effects. *Mar. Drugs* **2022**, *20*, 736. [CrossRef] [PubMed]

23. He, Z.H.; Xie, C.L.; Wu, T.; Yue, Y.T.; Wang, C.F.; Xu, L.; Xie, M.M.; Zhang, Y.; Hao, Y.J.; Xu, R.; et al. Tetracyclic steroids bearing a bicyclo [4.4.1] ring system as potent antiosteoporosis agents from the deep-sea-derived fungus *Rhizopus* sp. W23. *J. Nat. Prod.* **2023**, *86*, 157–165. [CrossRef]

24. He, Z.H.; Xie, C.L.; Wu, T.; Zhang, Y.; Zou, Z.B.; Xie, M.M.; Xu, L.; Capon, R.J.; Xu, R.; Yang, X.W. Neotricitrinols A-C, unprecedented citrinin trimers with anti-osteoporosis activity from the deep-sea-derived *Penicillium citrinum* W23. *Bioorg. Chem.* **2023**, *139*, 106756. [CrossRef] [PubMed]

25. Wang, F.D.; Yue, J.M. A total synthesis of (+)- and (−)-dihydrokavain with a sonochemical blaise reaction as the key step. *Eur. J. Org. Chem.* **2005**, *2005*, 2575–2579. [CrossRef]

26. Roberts, A.; Beaumont, C.; Manzarpour, A.; Mantle, P. Purpurolic acid: A new natural alkaloid from *Claviceps purpurea* (Fr.) Tul. *Fungal Biol.* **2016**, *120*, 104–110. [CrossRef] [PubMed]

27. Zhang, Z.; He, X.; Wu, G.; Liu, C.; Lu, C.; Gu, Q.; Che, Q.; Zhu, T.; Zhang, G.; Li, D. Aniline-tetramic acids from the deep-sea-derived fungus *Cladosporium sphaerospermum* L3P3 cultured with the HDAC inhibitor SAHA. *J. Nat. Prod.* **2018**, *81*, 1651–1657. [CrossRef] [PubMed]

28. Li, Y.Q.; Park, H.J.; Han, E.S.; Park, D.K. Inhibitory effect on B16/F10 mouse melanoma cell and HT-29 human colon cancer cell proliferation and cordycepin content of the butanol extract of *Paecilomyces militaris*. *J. Med. Plant Res.* **2011**, *5*, 1066–1071.

29. Domondon, D.L.; He, W.; De Kimpe, N.; Hofte, M.; Poppe, J. Beta-adenosine, a bioactive compound in grass chaff stimulating mushroom production. *Phytochemistry* **2004**, *65*, 181–187. [CrossRef]

30. Qiu, W.; Wu, J.; Choi, J.H.; Hirai, H.; Nishida, H.; Kawagishi, H. Cytotoxic compounds against cancer cells from *Bombyx mori* inoculated with *Cordyceps militaris*. *Biosci. Biotechnol. Biochem.* **2017**, *81*, 1224–1226. [CrossRef]

31. Tatani, K.; Hiratochi, M.; Nonaka, Y.; Isaji, M.; Shuto, S. Identification of 8-aminoadenosine derivatives as a new class of human concentrative nucleoside transporter 2 inhibitors. *ACS. Med. Chem. Lett.* **2015**, *6*, 244–248. [CrossRef] [PubMed]

32. Xue, Y.; Wu, L.; Ding, Y.; Cui, X.; Han, Z.; Xu, H. A new nucleoside and two new pyrrole alkaloid derivatives from *Cordyceps militaris*. *Nat. Prod. Res.* **2020**, *34*, 341–350. [CrossRef]

33. Youssef, D.T.A.; Badr, J.M.; Shaala, L.A.; Mohamed, G.A.; Bamanie, F.H. Ehrenasterol and biemnic acid; new bioactive compounds from the Red Sea sponge *Biemna ehrenbergi*. *Phytochem. Lett.* **2015**, *12*, 296–301. [CrossRef]

34. Ma, Y.T.; Qiao, L.R.; Shi, W.Q.; Zhang, A.L.; Gao, J.M. Metabolites produced by an endophyte *Alternaria alternata* isolated from *Maytenus hookeri*. *Chem. Nat. Compd.* **2010**, *46*, 504–506. [CrossRef]

35. Ying, Y.M.; Shan, W.G.; Liu, W.H.; Zhan, Z.J. Alkaloids and nucleoside derivatives from a fungal endophyte of *Huperzia serrata*. *Chem. Nat. Comd.* **2013**, *49*, 184–186. [CrossRef]

36. Kaaniche, F.; Hamed, A.; Abdel-Razek, A.S.; Wibberg, D.; Abdissa, N.; El Euch, I.Z.; Allouche, N.; Mellouli, L.; Shaaban, M.; Sewald, N. Bioactive secondary metabolites from new endophytic fungus *Curvularia.* sp isolated from *Rauwolfia macrophylla*. *PLoS ONE* **2019**, *14*, e0217627. [CrossRef]

37. Sun, Y.; Tian, L.; Huang, J.; Li, W.; Pei, Y.H. Cytotoxic sterols from marine-derived fungus *Pennicillium* sp. *Nat. Prod. Res.* **2006**, *20*, 381–384. [CrossRef] [PubMed]

38. Fang, S.T.; Wang, Y.J.; Ma, X.Y.; Yin, X.L.; Ji, N.Y. Two new sesquiterpenoids from the marine-sediment-derived fungus *Trichoderma harzianum* P1-4. *Nat. Prod. Res.* **2019**, *33*, 3127–3133. [CrossRef]

39. Dearman, R.J.; Cumberbatch, M.; Hilton, J.; Clowes, H.M.; Fielding, I.; Heylings, J.R.; Kimber, I. Influence of dibutyl phthalate on dermal sensitization to fluorescein isothiocyanate. *Fundam. Appl. Toxicol.* **1996**, *33*, 24–30. [CrossRef] [PubMed]

40. Zeiger, E.; Haworth, S.; Mortelmans, K.; Speck, W. Mutagenicity testing of di(2-ethylhexyl)phthalate and related chemicals in Salmonella. *Environ. Mutagen.* **1985**, *7*, 213–232. [CrossRef]

41. Wang, W.; Guo, J.; Zhang, J.; Liu, T.; Xin, Z. New screw lactam and two new carbohydrate derivatives from the methanol extract of rice bran. *J. Agric. Food. Chem.* **2014**, *62*, 10744–10751. [CrossRef]

42. Theil, F.; Schick, H. Enzymes in organic-synthesis. 5. An improved procedure for the regioselective acetylation of monosaccharide derivatives by pancreatin-catalyzed transesterification in organic-solvents. *Synthesis* **1991**, *22*, 533–535. [CrossRef]

43. Park, S.; Kazlauskas, R.J. Improved preparation and use of room-temperature ionic liquids in lipase-catalyzed enantio- and regioselective acylations. *J. Org. Chem.* **2001**, *66*, 8395–8401. [CrossRef] [PubMed]

44. Li, X.B.; Li, Y.L.; Zhou, J.C.; Yuan, H.Q.; Wang, X.N.; Lou, H.X. A new diketopiperazine heterodimer from an endophytic fungus *Aspergillus niger*. *J. Asian Nat. Prod. Res.* **2015**, *17*, 182–187. [CrossRef] [PubMed]
45. Yan, H.J.; Gao, S.S.; Li, C.S.; Li, X.M.; Wang, B.G. Chemical constituents of a marine-derived endophytic fungus *Penicillium commune* G2M. *Molecules* **2010**, *15*, 3270–3275. [CrossRef]
46. Tao, Y.; Feng, C.; Xu, J.; Shen, L.; Qu, J.; Ju, H.; Yan, L.; Chen, W.; Zhang, Y. Di(2-ethylhexyl) phthalate and dibutyl phthalate have a negative competitive effect on the nitrification of black soil. *Chemosphere* **2022**, *293*, 133554. [CrossRef]
47. Silvin, A.; Uderhardt, S.; Piot, C.; Da Mesquita, S.; Yang, K.; Geirsdottir, L.; Mulder, K.; Eyal, D.; Liu, Z.; Bridlance, C.; et al. Dual ontogeny of disease-associated microglia and disease inflammatory macrophages in aging and neurodegeneration. *Immunity* **2022**, *55*, 1448–1465. [CrossRef]
48. Orihuela, R.; McPherson, C.A.; Harry, G.J. Microglial M1/M2 polarization and metabolic states. *Br. J. Pharmacol.* **2016**, *173*, 649–665. [CrossRef]